Electrochemical copolymerization of aniline and para-phenylenediamine on IrO_2-coated titanium electrode

C.-H. YANG, T.-C. WEN*

Department of Chemical Engineering, National Cheng Kung University, Tainan, Taiwan 70101

Copolymerization of aniline (AN) and para-phenylenediamine (PPDA) was electrochemically performed by cyclic voltammetry on IrO_2-coated titanium electrodes in 0.5 M H_2SO_4. The cyclic voltammograms, with and without a middle peak at about 580 mV, can be produced by controlling the PPDA concentration in the aniline solution during polymer preparation. The peak at about 580 mV corresponds to the para-aminophenol/benzoquinoneimine (PAP/QI) redox couple and cross-linking sites. The mass of polymer deposited on an IrO_2-coated titanium electrode is correlated with the polymer anodic peak current, which allows the rates of polymer deposition to be monitored by increases in the anodic peak current at various PPDA concentrations. SEM photographs show that the morphology of the polymer film depends dramatically on PPDA concentration. Stability test information can be used in generating an effective index to discern between the crosslinking and the PAP/QI reactions induced by PPDA. The linear relationship between the second redox process potential $(E_{1/2})$, corresponding to the oxidation and reduction between polaronic emeraldine and pernigraniline in PPDA-modified PANI films, and pH, possesses a slope of about -120 mV/pH.

1. Introduction

The electrically conductive nature of the polyaniline (PANI) family has been well known for more than a century [1, 2]. These days, this family of compounds is considered as being one of the most promising conducting organic materials, due to their good environmental stability [3, 4], as well as their moderately high conductivity upon doping with simple Brønsted acids [3-6]. These compounds can be readily prepared using cyclic voltammetry through the electrochemical oxidation of aniline [7-12].

Members of the PANI family have been electrochemically deposited on platinum electrodes [10], giving electrochemically active thin films. The electrochemical behaviour of these films has been extensively investigated, with two main redox systems having been identified [3, 4, 11, 12]. The linear relationship between the second redox process potential, $E_{1/2}$, of PANI over the $-0.2-4$ pH range in HCl aqueous solution has also been studied [13, 14]. Cyclic voltammogram characteristics, especially those in the upper potential limit region and those of oxidative current density, depend upon conditions of electrochemical deposition. Cyclic voltammetric peaks, in addition to those at *ca.* 480 and 580 mV [15-17] (vs Ag/AgCl), are tentatively attributed to the formation of oligomers, crosslinking reactions, formation of phenazine rings and imine hydrolysis; the latter leading to the corresponding quinone [18].

The electrochemical polymerization of aniline has been described as a bimolecular reaction involving a radical cationic intermediate and a two-electron transfer process for each polymerization step [10, 19-21]. Recently, Wei *et al.* [22] systematically investigated the kinetics of aniline electrochemical polymerization. By correlating the amount of aniline deposited on a platinum electrode with anodic peak current during polymerization, they were able to monitor the rates of polymer deposition at various concentrations of aniline by increases in anodic peak current.

One of the most important characteristics of PANI films are their stability with respect to their reversible transition from the oxidized, conducting state to the reduced, nonconducting state [23]. It is well known that continuous cycling of PANI coated electrodes in electrolytes devoid of aniline results in destruction of the PANI coating [16, 24, 25].

The preparation conditions, in addition to the type of monomer and substrates employed, determine the properties and structures of the resulting polymeric film [26]. PANI film is generally deposited upon platinum, gold and graphite substrates. Although few metal oxide electrodes have been used as substrates for the formation of electrochemically active thin films [26, 27], iridium oxide (IrO_2) electrodes have been reported to be considerably more resistant to degradation in strong acids [28]. Moreover, an IrO_2 electrode exhibits a broad peak
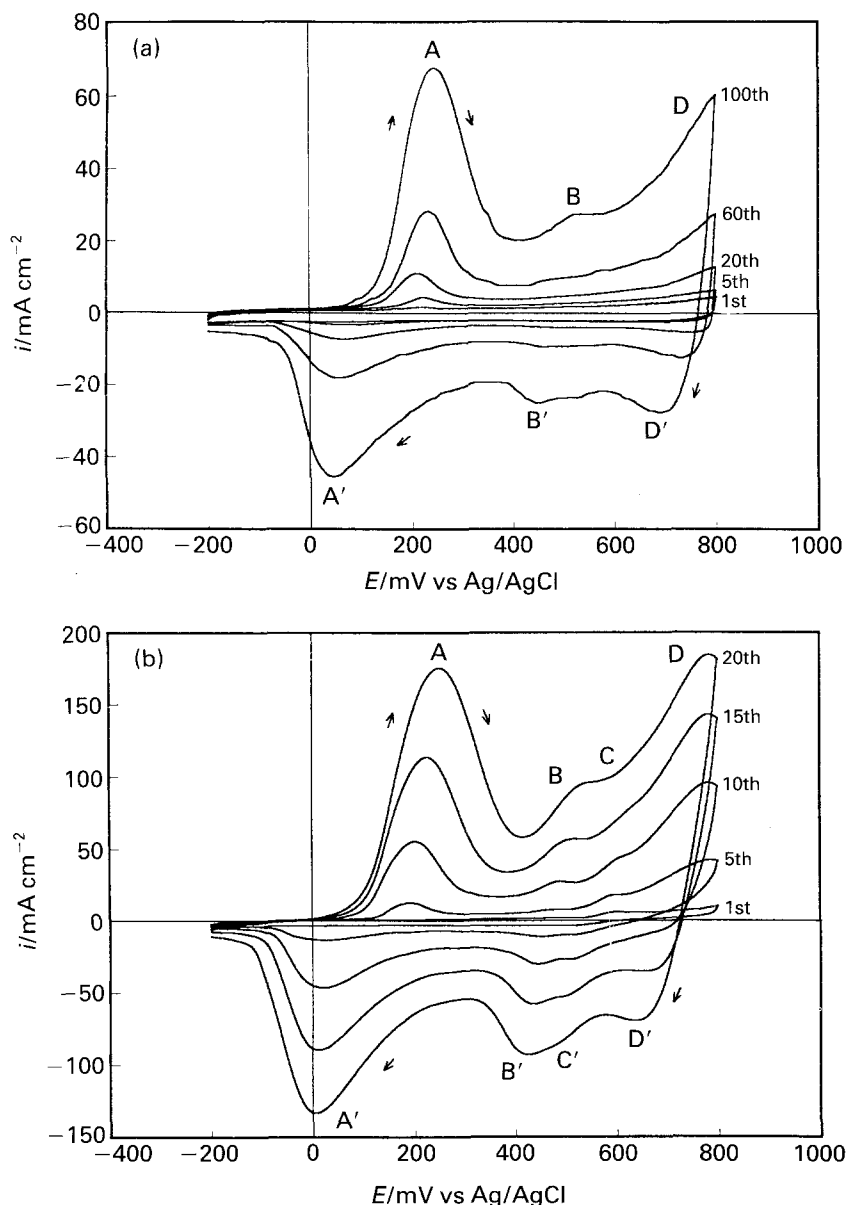
* To whom all correspondence should be addressed

Fig. 1. Consecutive cyclic voltammograms of PPDA-modified PANI films on an IrO₂-coated titanium electrode in 0.5 M H₂SO₄ at a scan rate of 50 mV s⁻¹. The films were prepared from the following solutions: (a) 0.2 M aniline; (b) 0.19 M aniline + 0.005 M PPDA; (c) 0.163 M aniline + 0.0185 M PPDA; (d) 0.1 M aniline + 0.05 M PPDA; (e) 0.066 M aniline + 0.067 M PPDA; (f) 0.005 M aniline + 0.075 M PPDA; and (g) 0.1 M PPDA.

corresponding to the Ir(III)/Ir(IV) redox transition between 0.5 and 1.0 V vs RHE [29]. This redox transition could possibly catalyse PANI polymer formation. This information, coupled with this laboratory's interest in metal-oxide electrodes, made IrO₂ the working electrode of choice for this study.

As the small amount of work done on para-phenylenediamine (PPDA)-modified PANI attests [27], small additions of PPDA to aniline solutions can impart a 'network-like' morphology to the polymer films and also increase the growth rate. For PPDA to be used in engineering applications such as rechargeable batteries and immobilization of catalytic sites, additional information regarding such quantitative information as polymeric growth rate and stability are of paramount importance.

The present work describes an investigation of the effect of PPDA addition on PANI film growth, with cyclic voltammetry being employed in the examination of the film electrochemical behaviour. Morphological changes and stability of the polymer films in 0.5 M H₂SO₄ are also examined.

2. Experimental details

2.1. Instrumentation and chemicals

Reagent grade aniline (Merck) was doubly distilled and the resulting colorless liquid kept under nitrogen in darkness at 5° C. Reagent grade para-phenylenediamine (Merck) was used without additional treatment. A 0.5 M solution of H₂SO₄ was prepared from concentrated H₂SO₄ (Merck). Electrochemical synthesis and cyclic voltammetry were performed on a BAS-100B (Bioanalytic System, Inc. USA). A three-electrode cell was utilized with an Ag/AgCl electrode (Argenthal, 3 M KCl, 0.207 V at 25° C) acting as reference and a platinum wire serving as counter electrode. The size of the IrO₂-coated titanium working electrode varied in each specific experiment. The minimum and maximum sizes used were 1 and 4 cm², respectively. A Luggin capillary, whose tip was set at a distance of about 1 mm from the surface of the working electrode, was used in minimizing errors due to iR drop in the electrolytes.
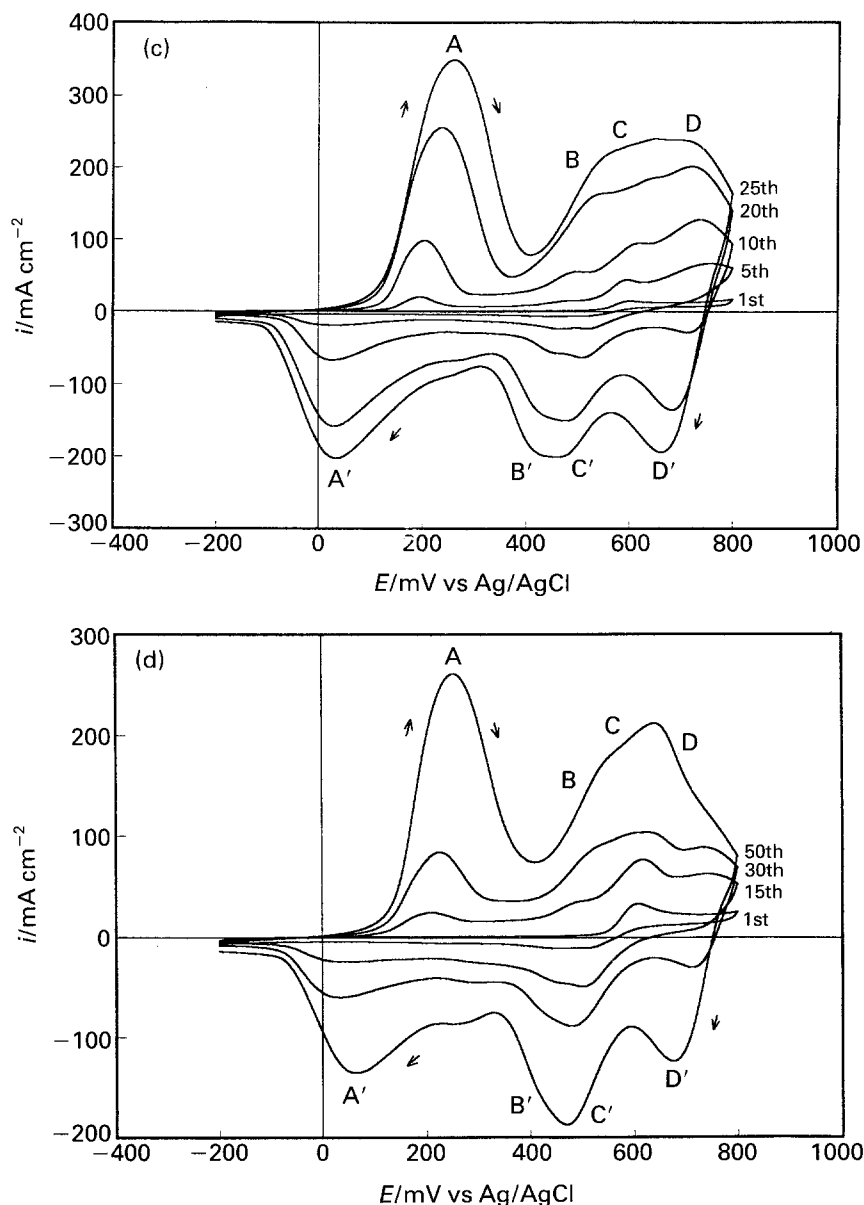
Fig. 1. (Continued).

All syntheses and measurements were performed under nitrogen and all potentials are quoted against Ag/AgCl.

2.2. Preparation of IrO_2-coated titanium electrode

The preparation of IrO_2-coated titanium electrodes was similar to that described earlier [29, 30]. IrO_2 was deposited by thermal decomposition on a titanium support ($20\,mm \times 20\,mm \times 1.2\,mm$). The starting solutions consisted of a total concentration of $0.25\,M$, $IrCl_3 \cdot xH_2O$ (Johnson Matthey) in an isopropanol solution containing 10% by volume concentrated HCl. After being dipped in their respective isopropanol solutions, the degreased and HCl-etched titanium supports were dried at $90°\,C$ for about 30 min. After drying, the supports were fired under air flow at $400°\,C$ for 10 min. This process was repeated five times and the final heating was carried out at the annealing temperature ($400°\,C$) for one hour. To minimize voltammetric charge differences

between the first and subsequent scans of each working electrode, six cyclic voltammograms were run in $0.5\,M$ aqueous H_2SO_4 at a scan rate of $50\,mV\,s^{-1}$ between -200 to $800\,mV$ before the electrode was used.

2.3. Polymer mass and anodic current correlation

PPDA-modified PANI was electrochemically deposited at $25°\,C$ by cyclic voltammetry on IrO_2-coated titanium electrodes ($4\,cm^2$) in $0.5\,M$ H_2SO_4 aqueous solutions containing constant normalities ($0.2\,N$) of $-NH_2$ ($0.2-0.066\,M$ aniline and $0-0.067\,M$ PPDA). The potential sweep, operating at a scan rate of $50\,mV\,s^{-1}$, covered the -200 to $800\,mV$ potential range. Reaction times, varying from 15 to 100 cycles, were chosen to control the amount of polymer deposited on the electrode. Cyclic voltammograms were taken after each PANI synthesis, from which the anodic current of the first oxidation peak occurring at about $200\,mV$ was measured.
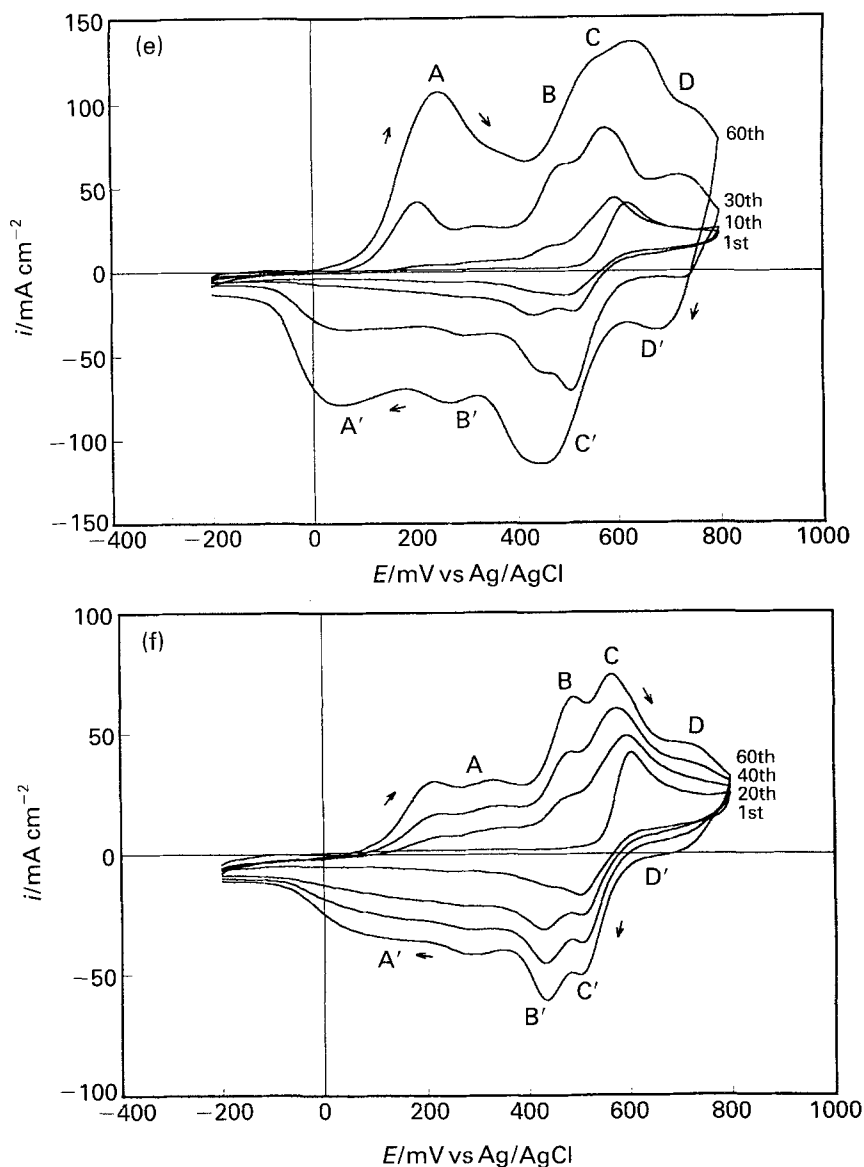
Fig. 1. (Continued).

The deposited aniline–para-phenylenediamine (AN–PPDA) copolymer film on the electrode was then washed with 0.5 M H_2SO_4 and dried under vacuum for 48 h. For each synthesis, polymer weight was determined by the difference in weight between the electrode with and without the deposited copolymer.

2.4. Effect of PPDA addition

AN–PPDA copolymer films were prepared on 1 cm² IrO_2-coated titanium electrodes as above at various deposition times. Cyclic voltammograms of the deposited polymer were obtained following the method of Wei et al. [22]. From the cyclic voltammograms of the polymerization process recorded simultaneously with the synthesis of the polymer (Fig. 1), the anodic faradaic current of the first oxidation peak at about 200 mV was measured by subtracting the small background current from the total anodic current. This net current was then plotted against the cycle number (the reaction time) and the results subjected to regression analysis. The rate of polymer deposition (the slope of net current

against cycle number) at any point was calculated by means of the associated polynomial regression equation.

2.5. SEM examination

Samples of AN–PPDA copolymer films were prepared on 1 cm² IrO_2-coated titanium electrodes as above at various deposition times. For SEM examination (JOEL JSM35), the PPDA-modified PANI films were removed from the cell, rinsed with 0.5 M H_2SO_4 and then finally dried in air.

2.6. Stability of AN–PPDA copolymer films

AN–PPDA copolymer films were prepared on 1 cm² IrO_2-coated titanium electrodes as above at various deposition times. Copolymer film stability was studied in 0.5 M H_2SO_4 devoid of AN and PPDA, following the method of Tsakova and Milchev [23]. Eighty continuous scans were run at a scan rate of 100 mV s⁻¹ between −200 and 800 mV at 25° C.
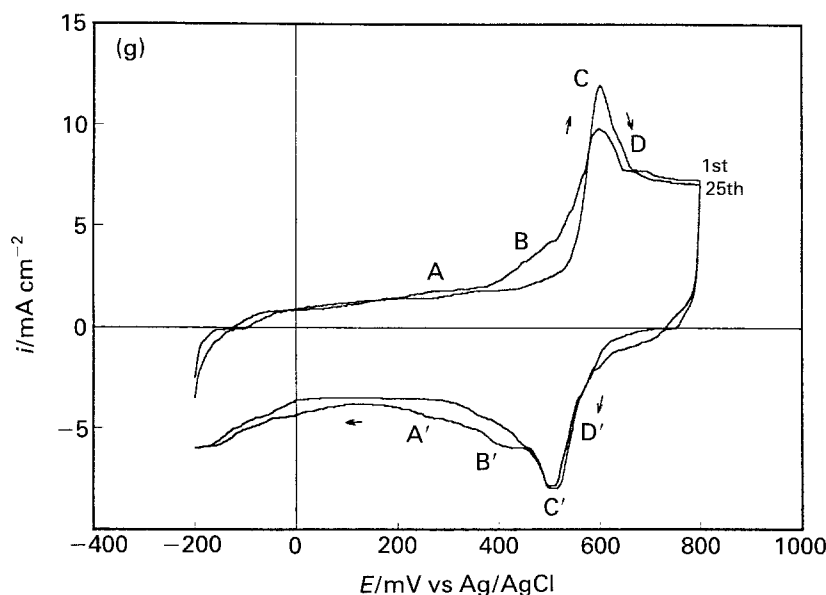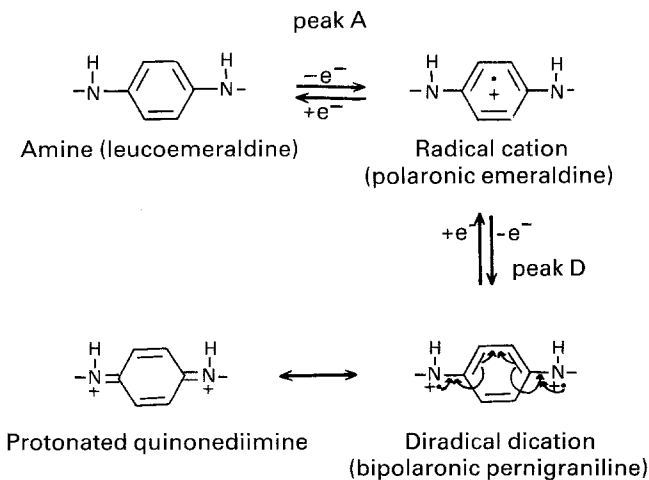
Fig. 1. (Continued).

3. Results and discussion

3.1. Cyclic voltammetry of copolymerization

A series of cyclic voltammograms (CVs) of AN-PPDA copolymerization of an IrO_2-coated titanium electrode in 0.5 M H_2SO_4 containing constant normalities of $-NH_2$ (0.2 N) are shown in Fig. 1. A typical CV indicative of pure AN polymerization is shown in Fig. 1(a). In the anodic sweep (refer to cycle 100), three major redox couples are distinguishable: the first, formation of radical cations (polaronic emeraldine), occurs between 210 and approximately 240 mV (peak A); the second, benzoquinone adsorption, occurs at about 420 and 500 mV (peak B); and the third, formation of diradical dications (represented by the resonance structures: bipolaronic pernigraniline and protonated quinonediimine), commences at approximately 600 mV, and reaches a maximum at 800 mV (peak D). In the cathodic sweep of cycle 100, the presence of three corresponding broad reduction peaks labelled: A', B', D'. In subsequent cycles, peaks A and D become more intense while a new oxidation peak, B, becomes apparent. The potential of peak A is originally present at

approximately 210 mV in the cycles 1–20, but shifts to slightly higher potentials in later cycles. This shift is attributed to the presence of oligomeric species adsorbed on the electrode surface [11, 12, 15, 17]. These oligomeric species are further polymerized in later sweeps. Two main redox couples, corresponding to peaks A and D, exist.

Glarum and Marshall [31] reported that in situ ESR signals were observed at both electrode potentials corresponding to CV peaks A and D for PANI films. Radical properties were detected between the two potential boundaries. These results were substantiated by the ESR studies of Stilwell and Park on PANI films [11], the mechanism of which, is represented by Scheme 1. Peak A, represented by the absorption maximum at 328 nm, corresponds to the leuco form (leucoemeraldine) of PANI film, which oxidizes into radical cations (the polaronic form of emeraldine). These cations possess an absorption maximum at 440 nm. Radical cations are generated upon oxidation which persist in PANI films until the potential reaches a value of about 600 mV (peak D). At peak D, diradical dications (the bipolaronic form of pernigraniline) are generated, which establish an equilibrium with their other resonance form,

peak A

Amine (leucoemeraldine)   Radical cation
                           (polaronic emeraldine)

peak D

Protonated quinonediimine   Diradical dication
                             (bipolaronic pernigraniline)
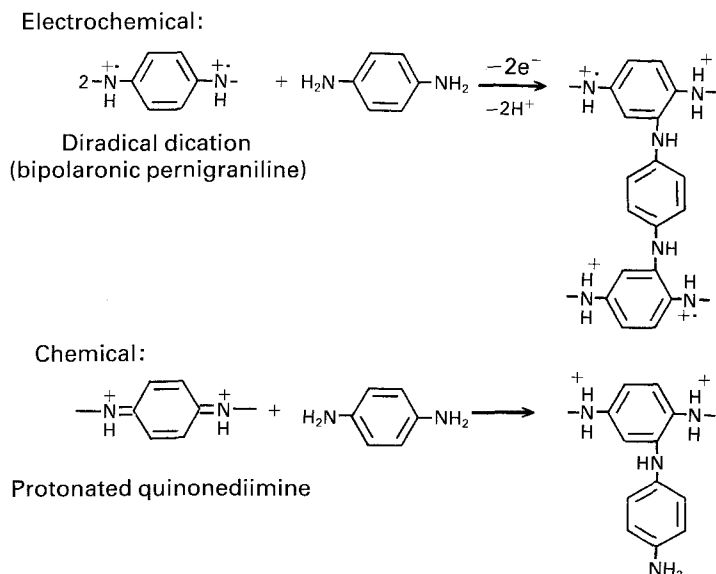
Scheme 1. The mechanism of the growing polyaniline.

protonated quinonediimine; results substantiated by Lapkowski et al. [32] and MacDiarmid et al. [33], who reported that in situ EPR signals were observed at electrode potentials corresponding to the A and D CV peaks. MacDiarmid et al. [33] reported that the positive charge on the nitrogen atoms will be unequally distributed over all nitrogen atoms in the polymer, with this positive charge being undoubtedly delocalized onto the C_6H_4 ring. When aromatic rings are present, thus, at potentials more positive than that at peak D, the formation of diradical dications play the most important role, allowing for further PANI growth, if aniline is present in the solution. This species is an energetic electrophile, extracting an electron from aniline, reveals becoming a radical cation, which bonds with another radical, indicating by the increase in the peak A intensity that these radical cations undergo coupling give the polymer deposited on the anode surface. The B/B′ peaks observed at about 480 mV, only appear at later sweeps (higher cycle numbers). The B/B′ peaks are assigned to the benzoquinone/hydroquinone (BQ/HQ) couple [11, 12], since their peak potentials occur in the same region as the BQ/HQ couple in 1 M H_2SO_4 and BQ/HQ is generated during AN-polymer film growth, becoming strongly adsorbed in the polymer matrix. Literature evidence [11, 17, 33] suggests that peak B arises from the oxidation product (BQ) of the imine hydrolysis reactions, while peak B′ arises from the reduction product (HQ).

The CV corresponding to 0.005 M PPDA addition is shown in Fig. 1(b). Its shape is similar to that of Fig. 1(a), peak A currents are larger and have shifted to lower potentials (175–200 mV), suggesting that polymer deposition on the electrode surface is responsible for the acceleration of AN–PPDA electrochemical copolymerization. This situation is thought to arise from PPDA addition inducing quinonediimine formation, which results in a significant increase in the nucleation rate of polymer deposition. In comparison to Fig. 1(a), an additional middle peak, C, appears ca. 580 mV in Fig. 1(b).

This peak attributed to a crosslinking site and para-aminophenol/benzoquinone-imine side reaction (PAP/QI) induced by the diamine (PPDA) during copolymerization [11, 17]. Moreover in Fig. 1(b), peak D shifts to a lower potential at earlier sweep cycles than in Fig. 1(a), suggesting that the PPDA addition facilitates quinonediimine formation.

The CV corresponding to 0.0185 M PPDA addition is shown in Fig. 1(c). In comparison to the previous two runs, peak A currents in the 165 to 200 mV potential region are larger and that peak D shifts to lower potentials at earlier sweep cycles. An examination of Fig. 1(a), (b) and (c) reveals the tendency for PPDA to act as an accelerator for AN–PPDA copolymerization, and that PPDA addition has increased the nucleation sites, thereby increasing the AN–PPDA copolymerization rate. In Fig. 1(c), peak C is relatively more obvious than in Fig. 1(b). As a direct result of the fact that quinonediimine formation is more facile for PPDA than for AN (see below), peak C is thought to represent PPDA induced crosslinking sites and the PAP/QI side reaction. The high number of PANI units in the polymer provide many branched points for cross-linkage with PPDA, the mechanism of which, is represented by Scheme 2. According to Stilwell and Park's experiments [11], concerning electrochemical or chemical branched additions within PANI chains, the site for monomer addition to, C_6H_4 rings is within the growing PANI chain. This results in a branched product that could conceivably crosslink with other chains.

The above discussion presents a number of easily obtained changes in the CV of AN–PPDA copolymerization with PPDA addition, suggesting that the electrochemical behaviour of these films are linked to the amount of PPDA added. In order to gain a further understanding of this effect, PPDA was added to the equivalence point of $-NH_2$ (AN) and a CV then run. A typical CV is presented in Fig. 1(d). In comparison with Figs. 1(a)–(c), the peak A currents of Fig. 1(d) are smaller than those in Fig. 1(b) and (c) but larger than that in Fig. 1(a). A

Electrochemical:

Diradical dication
(bipolaronic pernigraniline)

Chemical:

Protonated quinonediimine

Scheme 2. Chemical or electrochemical additions within the polyaniline chain.

comparison of Fig. 1(c) and (d) reveals that addition of higher concentrations of PPDA leads to an increase in C/C' peak currents; or, in other words, to a simultaneous increase in crosslinking sites and the PAP/QI side reaction [11, 27]. One possible explanation for this behaviour is that at high concentrations, excess PPDA enters into the aforementioned side reactions. In addition, peak D in Fig. 1(d), shifts to lower peak potentials at earlier sweep cycles than in Fig. 1(c), suggesting that this shift is proportional to PPDA addition. This situation is thought to arise from the more facile formation of quinonediimines over aniline polymerization at higher PPDA concentrations.

The CV resulting from PPDA concentrations larger than $-NH_2$ (AN) normality is presented in Fig. 1(e). In comparison to Fig. 1(d), peak A currents are smaller, and shifted to higher potentials (220–250 mV), and that the C/C' peaks are more intense. The C/C' peaks are assigned to the para-aminophenol/benzoquinone-imine (PAP/QI) couple, since their peak potentials occur in the same region as the PAP/QI couple in 0.5 M H_2SO_4 and PAP/QI is generated during AN-polymer film growth, becoming strongly adsorbed in the polymer matrix. In contrast to Fig. 1(d), peak A shifts to higher potentials; acceptable results if we assume that peak A is depressed. These results lend further support to our supposition that the PAP/QI reaction is predominant under PPDA additions in excess of aniline $-NH_2$ normality.

The CV corresponding to 0.075 M PPDA is shown in Fig. 1(f). Many differences exist in comparison with previous runs. Foremost among these is the depression of peaks A/A' and the shift to lower potentials of peaks D/D' to such an extent that they now overlap peaks C/C'; results suggesting that quinonediimine is easily hydrolyzed to PAP/QI. In contrast, peaks B/B' and C/C' are enhanced, suggesting increased formation of such hydrolytic products as BQ/HQ and PAP/QI, respectively.

Evidently, the PAP/QI reaction is the predominant process controlling the observed CV behaviour.

A CV 0.1 M PPDA in 0.5 M H_2SO_4 at 50 mV s^{-1} scan rate is shown in Fig. 1(g). In the anodic sweep of cycle 1, the current density of peak D is larger than that of peak A, indicating that PPDA is easily oxidized into diradical dications. The diradical dications are protonated quinonediimine and/or bipolaronic pernigraniline, the D/D' peaks shift to less positive potentials, overlapping, and becoming indistinguishable from, peaks C/C'. These results suggest that the diradical dication is an energetic electrophile, and that is either easily hydrolyzed to PAP/QI or extracts an electron from a neighbouring C_6H_4 ring, thereby forming branched products. In comparison cycle 1, after 25 cycles, the A/A' and D/D' peaks have not increased in intensity. This observation strongly suggests that the growth of PANI film does not consist of the simple buildup of layers on the electrode surface as a result of PPDA oxidation products. Also in comparison to cycle 1, peaks C/C' (PAP/QI) have decreased, while peaks B/B' (BQ/HQ) have increased, indicating that the former has partially hydrolyzed to the latter and that these species have strongly adsorbed on the electrode.

The first cycle CV of 0.2 M aniline and 0.1 M PPDA in 0.5 M H_2SO_4 50 mV s^{-1} is shown in Fig. 2. A comparison of 1st cycle CVs of 0.1 M PPDA and 0.2 M AN, reveals that peak D commences at a less positive potential ($\sim$ 580 mV) for 0.1 M PPDA, indicating that PPDA is more easily oxidizable than AN. From our discussion, PPDA facilitates quinonediimine (protonated quinonediimine) formation in growing PANI films.

3.2. Correlation of deposited polymer mass with anodic current

The masses of AN–PPDA copolymer films deposited on IrO_2 electrodes against various i_ps (peak A values
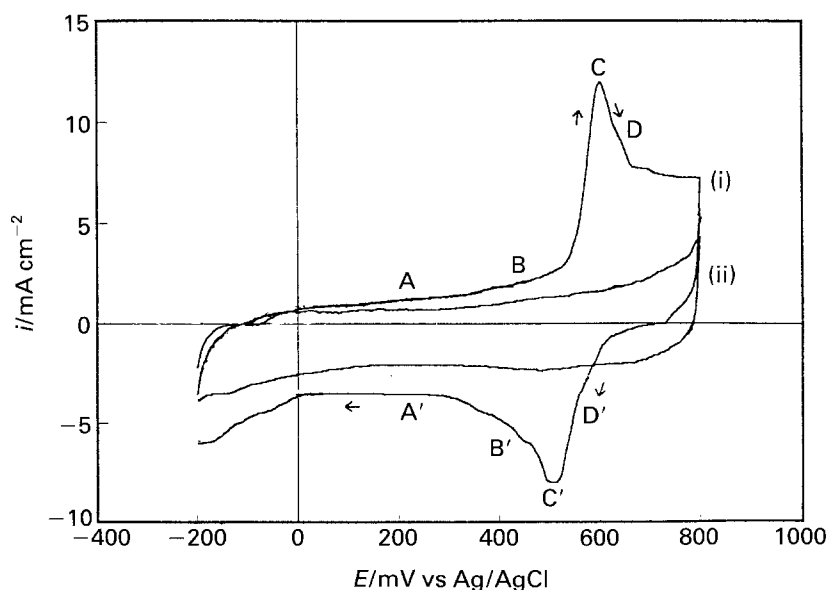

Fig. 2. A comparison of 1st cyclic voltammogram between 0.1 M PPDA (i) and 0.2 M aniline (ii) on an IrO_2-coated titanium electrode in 0.5 M H_2SO_4 at a scan rate of 50 mV s^{-1}.
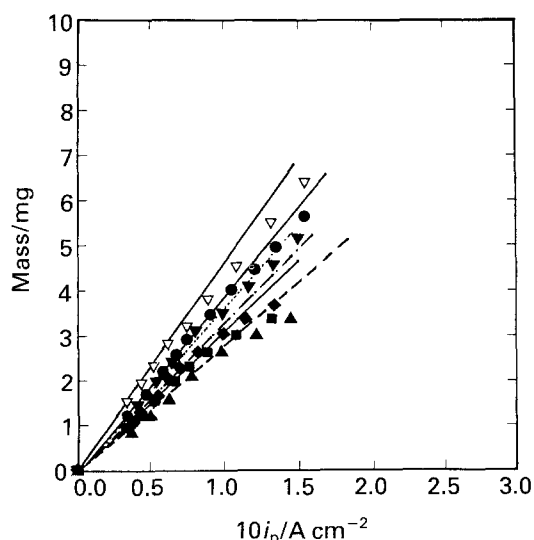
Fig. 3. A plot of the copolymer mass (film) deposited on an IrO_2-coated titanium electrode against polymer anodic peak current at about 200 mV. The films were prepared from the following solutions: (●) 0.2 M aniline; (▼) 0.199 M aniline + 0.0005 M PPDA; (■) 0.19 M aniline + 0.005 M PPDA; (▲) 0.163 M aniline + 0.0185 M PPDA; (◆) 0.1 M aniline + 0.05 M PPDA; and (▽) 0.066 M aniline + 0.067 M PPDA.

Fig. 4. Dependence of the anodic peak current on cycle number at various aniline and PPDA concentrations. A scan rate of $50 \, mV \, s^{-1}$ was used. Symbols are as in Fig. 3.

at $\sim$ 200 mV) were measured and are plotted in Fig. 3. At current densities lower than about $80 \, mA \, cm^{-2}$, anodic current is directly proportional to the amount of polymer formed, with the slope of this line seemingly dependent upon PPDA addition. These lower slope results, in comparison to the amount of polymer formed with PANI, may be due to thrusting of the growing species (oligomers) away from the electrode. These oligomers were green in colour and actually detached from the IrO_2 electrode during copolymerization, being observed as a green cloud encircling the electrode following detachment. Negative deviations from all lines above about $80 \, mA \, cm^{-2}$ are attributable to the presence of the oligomeric species adsorbed on the electrode surface [11, 15, 17]. Below current densities of about $80 \, mA \, cm^{-2}$, however, the amount of polymer deposited and i_p are in direct proportion. This relationship enables the amount of polymer deposited to be measured and the rate of polymer deposition to be determined. Similar linear relationships between polymer mass and i_p have been reported in PANI [22] and polypyrrole systems [34].

3.3. Effect of PPDA on copolymerization rate

The linear relationship between the amount of AN–PPDA copolymer deposited to anodic current, where anodic current is used directly to monitor the amount of polymer deposited on the electrode, is of great significance for a further understanding of the rate of PPDA-modified PANI deposition. Anodic current (i.e. the amount of polymer deposited) as a function of cycle number (i.e. the reaction time), at different PPDA concentrations is shown in Fig. 4. From an examination of Fig. 4, it is clear that the rate of polymer deposition depends significantly on
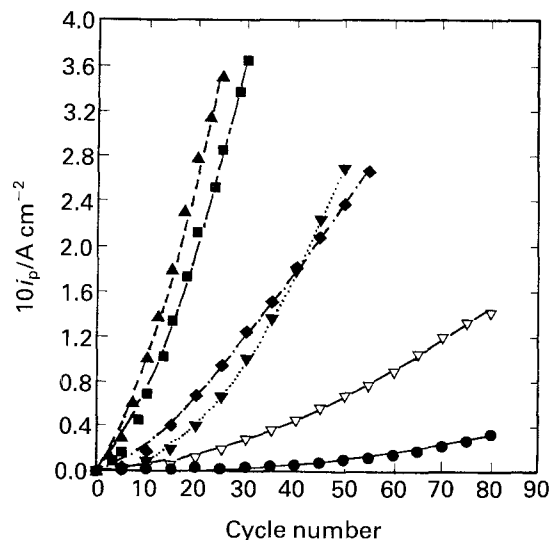
the amount of PPDA added. At PPDA concentrations less than 0.0185 M, the rate of copolymerization increases, while at concentrations larger than 0.05 M, the converse is true. The slope at any point on these curves gives the rate of polymer formation at the corresponding reaction time [22].

In Fig. 5, the rates of polymer deposition, derived from the slopes of the curves in Fig. 4, are plotted against anodic current values (i.e. the amount of polymer deposited) at various PPDA concentrations. In Fig. 5, the only straight line is exhibited by pure AN polymerization, indicating that this polymerization rate is first order with respect to AN concentration and possesses similar autoacceleration behaviour to that reported by Wei et al. in his study on pure AN polymerization [22]. In early cycles, at PPDA concentrations less than 0.0185 M, these curves exhibit saturated curve characteristics that imply acceleration of copolymerization by PPDA. This situation is thought to arise from PPDA addition facilitating formation of nucleation sites on the electrode
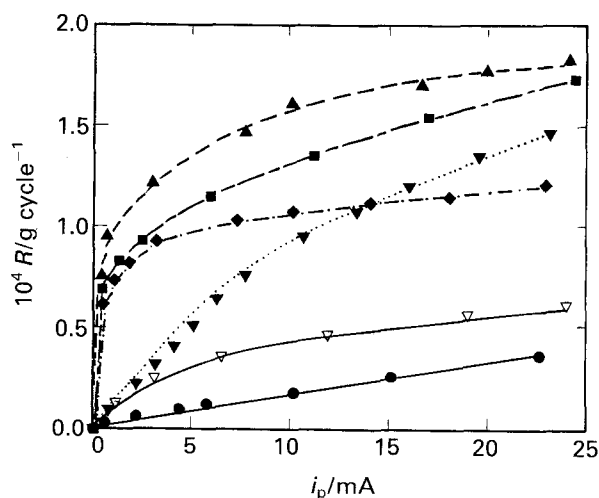

Fig. 5. Rate of polymer formation (values obtained from Fig. 3 slope measurements) at various PPDA concentrations against various anodic peak current values. Symbols are as in Fig. 3.

surface. The significant increase in reaction rates following polymer formation is due to polymer-mediated enhanced electron-transfer. At later cycles, copolymerization slows down due to oligomer formation and their subsequent adsorption on the electrode. Oligomer coverage of the electrode would be expected to depress an increase in the copolymerization rate at higher i_p values, corresponding to thicker polymer film formation; expectations in agreement with the saturated curve characteristics. At PPDA concentrations larger than 0.05 M (i.e., the equivalence point of $-NH_2$ (AN)), these saturated curve characteristics (in later cycles) and the nucleation rate of polymer deposition (in early cycles) are depressed. This situation is thought to arise from PPDA addition, which results in significant side reactions (for example BQ/HQ and PAP/QI) during polymerization, leading to a depression in the deposition rate due to the polymer chain failing to link. These results are the direct opposite of those early cycle results for PPDA concentrations of less than 0.0185 M.

3.4. Polymer morphology

The previous discussion highlighted facile changes in the CVs and deposition rates of AN–PPDA copolymerization with PPDA addition, inferring that these effects may be related to the polymer-deposition structure resulting from the particular PPDA addition in question. For an understanding of this influence, scanning electron microscopy was used in order to generate structural information on the polymer films resulting from the following growth solutions: 0.2 M AN, 0.199 M AN + 0.0005 M PPDA, 0.163 M AN + 0.0185 M PPDA, and 0.066 M AN +0.067 M PPDA. The resulting PANI films on IrO_2 electrodes are shown in Fig. 6(a)–(h).

At the beginning of deposition (20th cycle; Fig. 6(a)) for the 0.2 M aniline case, the polymer exhibits a rather uniform globular microstructure, whereas at the 80th cycle, a thicker, fibrous structure develops that exhibits some branching (Fig. 6(b)). Similar microstructures have been previously reported for PANI films prepared in the presence of H_2SO_4 or HCl [15, 27, 35]. In contrast to the initial globular deposit, the fibrous deposit is not entirely uniform over the electrode, which seems to indicate that the fibres are preferred sites for further polymer growth [27]. At the 20th cycle, in comparison with Fig. 6(a), Fig. 6(c), where 0.0005 M PPDA has been added, the resulting PPDA-modified PANI film is more uniform on the electrode surface. If the experiment is continued, a thicker, more porous film results at 40 cycles (Fig. 6(d)).

As the PPDA content is increased in the growth solution, the number of porous structures increase and cracks become larger on the polymer film. An examination of Fig. 6(e)–(f) reveals that the fibres are much thinner than those in Fig. 6(a)–(d) and they exhibit more branching; results indicating that PPDA may act as a crosslinking agent in its

modification of polymer film morphology. Since a PPDA molecule can bridge neighbouring fibres by coupling PANI at the ortho and meta positions, it may influence the growth mechanism of the polymer film (cf. Figs 4 and 5), promoting nucleation sites, leading to thinner fibres and more branching points [27]. At PPDA concentrations smaller than 0.0185 M, C/C' peaks arise from cross-linking sites induced by diamine (PPDA) during polymerization; results substantiated by SEM micrographs.

At PPDA concentrations greater than 0.05 M, a poorly adhering deposit was obtained on the electrode after polymerization. In the SEM micrographs of these films (cf. Fig. 6(g)–(h)), the absence of fibres and the distinct 'coral-like' morphology. Obviously PPDA dramatically influences polymer morphology. The C/C' peaks in the CV are attributable to PAP/QI species induced by diamine (PPDA) during polymerization, leading to a depression of the growth rate (cf. Figs 4 and 5) due to the polymer chain failing to link.

3.5. Effect of PPDA on film stability

A stable conductive polymer is very important for such practical applications as the rechargeable battery and in potential switching applications [15, 16, 23]. The stability of a particular PANI film was evaluated by a comparison of the 80th CV cycle with that of the 1st [16, 24, 25]. Eighty continuous scans between -200 and 800 mV at a scan rate of $100\,mV\,s^{-1}$ were used in the stability tests. The initial voltammograms of various PPDA-modified PANI films and those after 80 scans in 0.5 M H_2SO_4 are shown as 1 and 2, respectively, in Fig. 7(a)–(c). An examination of these figures reveals that differences in the resulting $i(E)$ profiles exist mainly in the 500–800 mV potential region. The stability test for the PANI film of Fig. 7(a) is similar to that reported previously by Tsakova and Milchev [23]. Also the shapes of Fig. 7(a) and (b) are not at all similar; the latter represents crosslinking reactions possibly induced by PPDA during copolymerization. This postulation is supported by the presence of peak C in Fig. 7(b) after stability testing. In Fig. 7(c) (0.067 M PPDA), on the other hand, peak C is absent after stability testing, indicating that the PAP/QI reaction is predominantly influenced by PPDA addition. In this instance, since the polymer cannot be linked to any further extent, the film is considered to be easily degradated.

In this study, polymer film stability was indexed by the following relative decrease relationship: $RD = (Q_i - Q_f)/Q_i$, where Q_i and Q_f represent the redox charges (500–800 mV) in the initial and final voltammograms, respectively. The stability data (RD), obtained for polymer films at various PPDA concentrations in the growth solution, are presented in Fig. 8. The lowest stability value (i.e. higher RD) consistently occurs at the initiation of polymerization. This result can be ascribed to the relatively
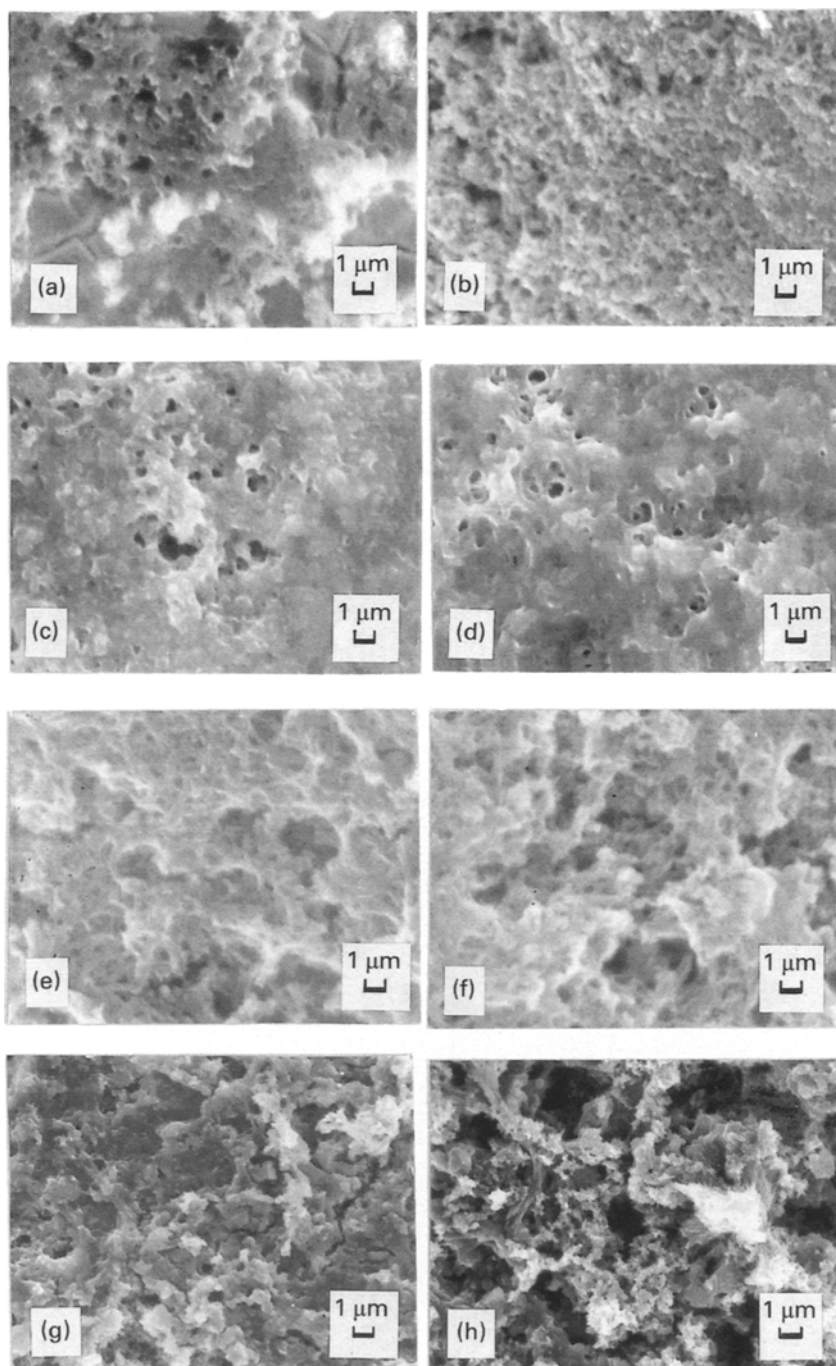
Fig. 6. SEM micrographs of the PPDA-modified PANI films grown on an IrO_2-coated titanium electrode in the following solutions: (a) 0.2 M aniline (20 cycles); (b) 0.2 M aniline (80 cycles); (c) 0.199 M aniline + 0.0005 M PPDA (20 cycles); (d) 0.199 M aniline + 0.0005 M PPDA (40 cycles); (e) 0.163 M aniline + 0.0185 M PPDA (5 cycles); (f) 0.163 M aniline + 0.0185 M PPDA (25 cycles); (g) 0.066 M aniline + 0.067 M PPDA (20 cycles); and (h) 0.066 M aniline + 0.067 M PPDA (80 cycles).

facile degradation of the initially deposited oligomer on the electrode during the cycling procedure. Average RDs for polymer films, calculated from Fig. 8 (without the first value in each case), were 33, 24, 25, 28, 36, and 41% for 0.2 M AN, 0.199 M AN + 0.0005 M PPDA, 0.19 M AN + 0.005 M PPDA, 0.163 M AN + 0.0185 M PPDA, 0.1 M AN +0.05 M PPDA, and 0.066 M AN + 0.067 M PPDA growth solutions, respectively. A marked decrease in RD was found for polymer films whose growth solutions contained 0.0005–0.0185 M PPDA, indicating that the stability of these films, in comparison with that of PANI film, can be promoted about 10%. As already discussed, for polymer films whose growth solutions contained 0.0005–0.0185 M PPDA, a cross-linking reaction no doubt accounts for the increased stability. At PPDA concentrations higher than

0.05 M, while RD increases with increasing PPDA concentration, film stability is reduced. At high PPDA concentrations, the subsequent side reactions are sufficiently rapid such that a higher oxidation state of PPDA (i.e. diimine) − most likely PAP/QI formation − leads to a polymer film that is easily degradated.

Since PPDA-modified PANI films degradated to the same products as PANI films, it is likely that degradation of the former during the cycling treatment follows a mechanism similar to that proposed by Stilwell and Park [16].

3.6. Redox process of polymer film

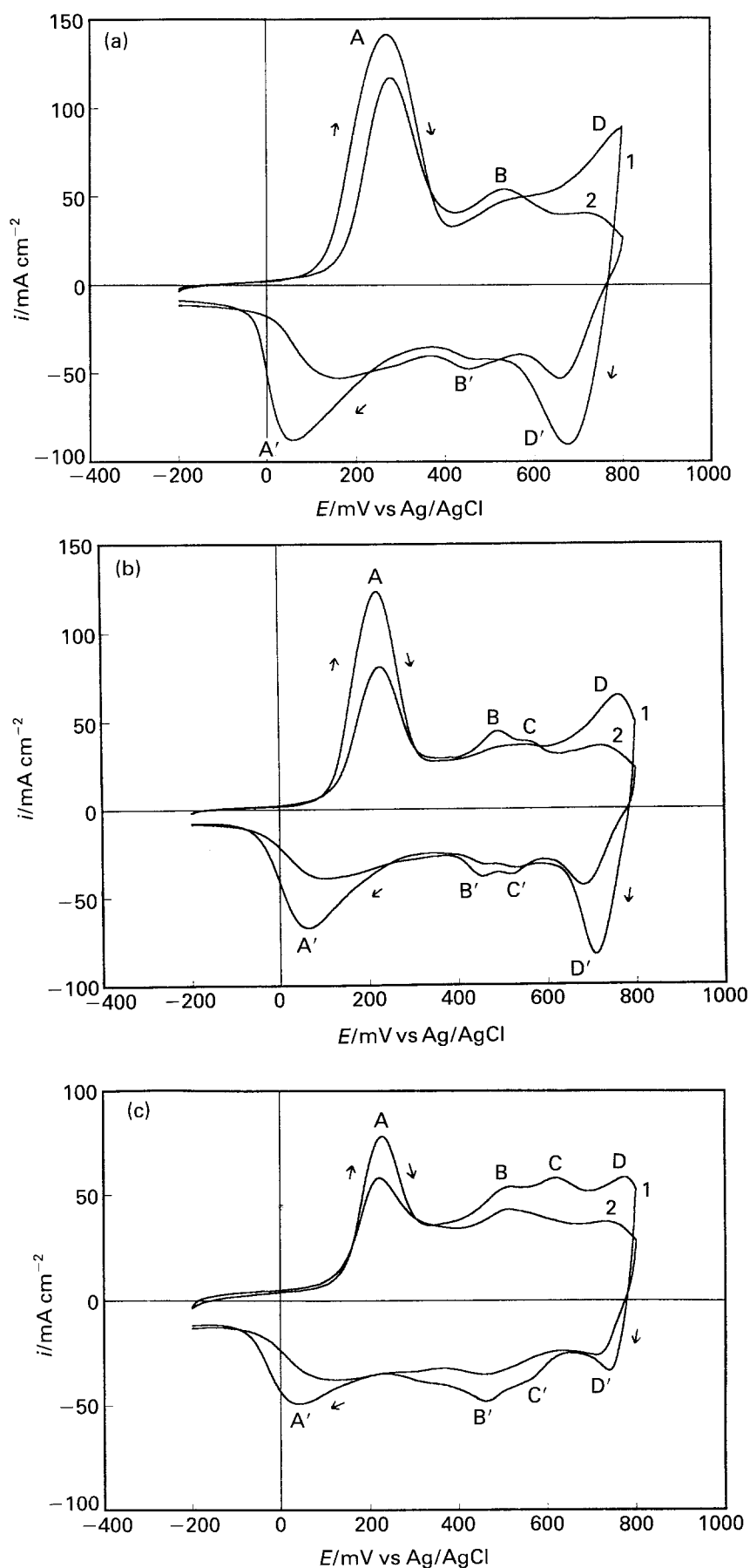Typical voltammograms obtained in 0.5 M H_2SO_4 at 0 pH of PANI and PPDA-modified PANI films

Fig. 7. Voltammetric curves of the PPDA-modified PANI films prepared from the following solutions: (a) 0.2 M aniline; (b) 0.199 M aniline + 0.0005 M PPDA; and (c) 0.066 M aniline + 0.067 M PPDA. Initial curves (1) and after 80 scans (2) in 0.5 M H_2SO_4 at a scan rate of 100 mV s^{-1}.

prepared from 0.2 M aniline, 0.19 M aniline + 0.005 M PPDA, 0.163 M aniline + 0.0185 M PPDA and 0.1 M aniline + 0.05 M PPDA are shown in Fig. 9. The well-resolved A/A′ and D/D′ peaks corresponding,

respectively, to the two following reversible redox processes: emeraldine and polaronic emeraldine; polaronic emeraldine and pernigraniline. The structural formulae of these species are shown in Scheme
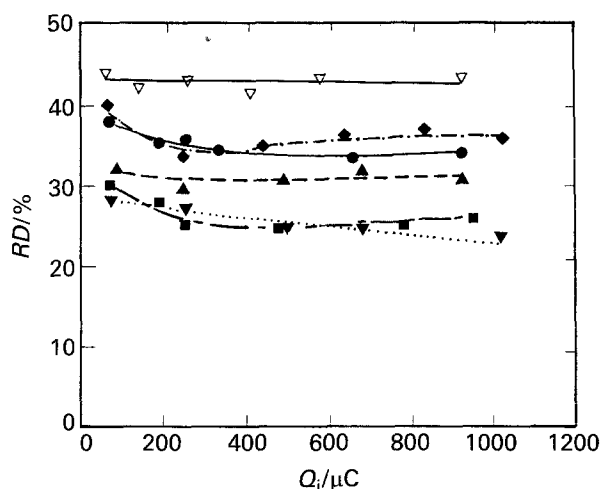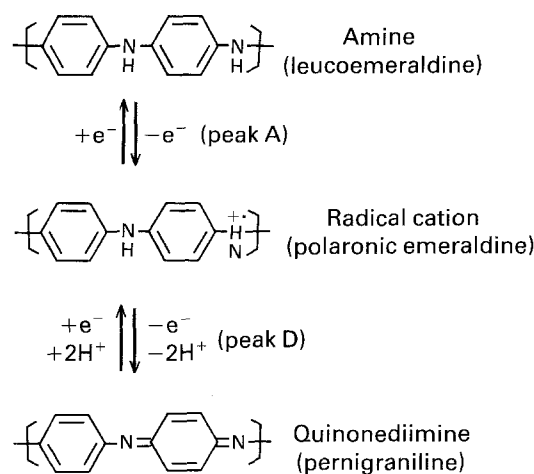
Fig. 8. Plot of *RD* values against Q_i (redox charge as deposited). Symbols are as Fig. 3.

Scheme 3. Structural formulae for dimeric repeating units used in rationalizing the electrochemistry of the redox couple corresponding to peaks A and D in Fig. 9. Note that the first and third species can exist in various protonated forms that are not shown here [14].

3. The potential of peak A associated with the emeraldine oxidation state of PANI does not change in the −0.1 to 1.5 pH range. Therefore, oxidation and reduction occur with no loss or gain of protons [14]. Moreover, the second redox process $(E_{1/2})$ associated with the D/D' peak potentials for both PANI and PPDA-modified PANI films is independent of the scan rate; results consistent with those of MacDiarmid *et al.* [13] and Wei *et al.* [14]. Our results of the second redox process $(E_{1/2})$ associated with the D/D' peak potentials against pH are shown in Fig. 10. In Fig. 10, the linear relationship between $E_{1/2}$ and pH for PANI and various PPDA-modified PANI films. All lines possess a slope of approximately −120 mV/pH, suggesting that morphological changes as a result of different PPDA content in polymer films do not significantly influence the second redox process. As the second redox process $E_{1/2}$ of PPDA-modified PANI films commences at a less positive potential than that of PANI film, it is quite possible that structural changes are responsible. Referring to Scheme 3, the second redox process

leads to the fully oxidized form of the polymer (pernigraniline) [13, 14]. The oxidation process results in deprotonation and consequently the formal potential $(E_{1/2})$ for this process decreases with increasing pH. As the oxidation mechanism proposed in Scheme 3 involves twice the number of protons as electrons, the Nernst equation predicts an $E_{1/2}$ against pH slope of −118 mV/pH at 25° C; results consistent with those obtained experimentally.

4. Conclusions

PPDA-modified PANI film was deposited on IrO₂-coated titanium electrodes, with the growth rate being strongly dependent on the concentration of PPDA in the growth solution. At PPDA concentrations lower than 0.0185 M, the rate of polymer formation on an IrO₂-coated titanium electrode increased with increasing PPDA concentration, while at concentrations larger than 0.05 M, the polymer film growth rate was depressed. In comparison to growing
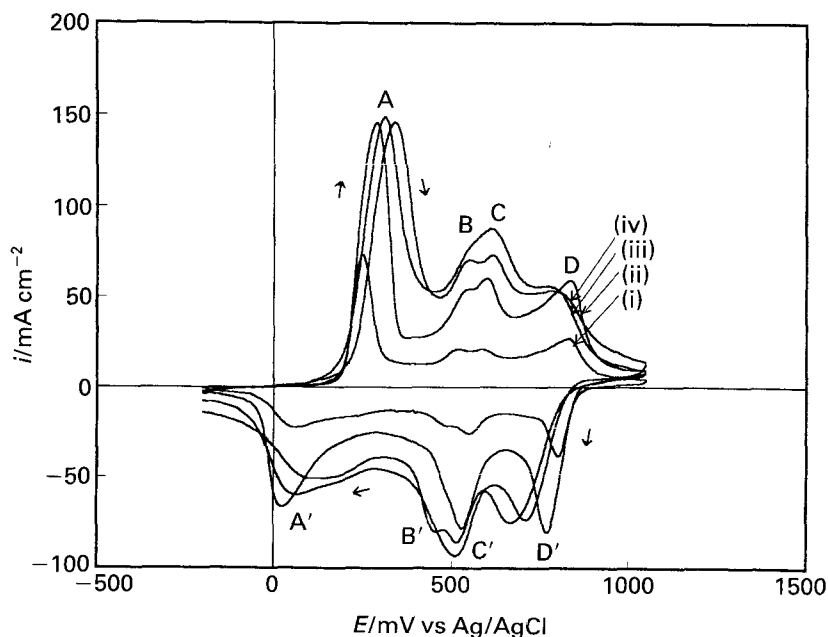

Fig. 9. Voltammetric curves of the PANI and PPDA-modified PANI films prepared from the following solutions: (i) 0.2 M aniline; (ii) 0.19 M aniline + 0.005 M PPDA; (iii) 0.163 M aniline + 0.0185 M PPDA; and (iv) 0.1 M aniline + 0.05 M PPDA; in H₂SO₄ aqueous solution (pH 0) at a scan rate of 100 mV s⁻¹.
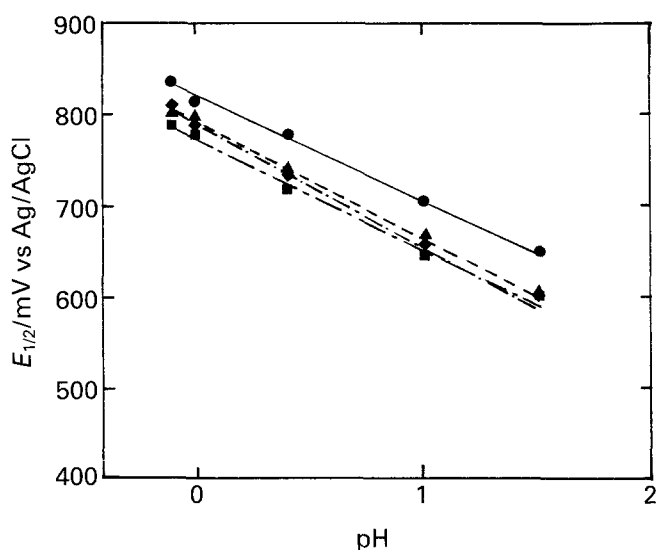
Fig. 10. Relationship between the second redox process potential ($E_{1/2}$), corresponding to the oxidation and reduction between polaronic emeraldine and pernigraniline in PPDA-modified PANI films, and pH (H_2SO_4 aqueous solution). Slope: (●) −116; (■) −122; (▲) −125; and (◆) −124. Symbols correspond to the respective growth solutions shown in Fig. 3.

PANI film, the growing PPDA-modified PANI film demonstrated additional middle peak CV character-istics (about 580 mV). At PPDA concentrations lower than 0.0185 M, crosslinking reactions and the PAP/QI side reaction occur simultaneously, with the former predominating. At PPDA concentrations larger than 0.05 M, the same situation occurs, but with the side reaction predominating. Polymer stab-ility (RD) also reflected the combined characteristics of both the crosslinking reaction (RD = 25%) and the PAP/QI reaction (RD = 40%). SEM results revealed that a 'network-like' structure results from the crosslinking reaction, while a 'coral-like' struc-ture develops when the PAP/QI reaction dominates. The linear relationship between the second redox pro-cess potential ($E_{1/2}$), corresponding to the oxidation and reduction between polaronic emeraldine and pernigraniline in PPDA-modified PANI films, and pH, with a slope of about −120 mV/pH, demon-strates that PPDA content does not significantly influence the second redox process.

Acknowledgement

References

[1]   H. Letheby, J. Chem. Soc. 15 (1862) 161.
[2]   A. G. Green and A. E. Woodhead, ibid. 97 (1910) 2338.
[3]   A. G. MacDiarmid, J. C. Chiang, M. Halpern, W. S. Huang, S. L. Mu, N. L. D. Somasiri, W. Wu and S. I. Yaniger, Mol. Cryst. Liq. Cryst. 121 (1985) 173.
[4]   J. C. Chiang and A. G. MacDiarmid, Synth. Met. 13 (1986) 193.
[5]   R. De Surville, M. Jozefowicz, L. T. Yu, J. Perichon and R. Buvet, Electrochim. Acta 13 (1968) 1451.

[6]   E. W. Paul, A. J. Ricco and M. S. Wrighton, J. Phys. Chem. 89 (1985) 1441.
[7]   E. Genies and C. Tsintavis, J. Electroanal. Chem. 195 (1985) 109.
[8]   A. Thyssen, A. Bogerding and J. W. Schultze, Makromol. Chem., Macromol. Symp. 8 (1987) 143.
[9]   U. Koenig and J. W. Schultze, J. Electroanal. Chem. 242 (1988) 243.
[10]   A. Diaz and A. Logan, ibid. 111 (1980) 111.
[11]   D. E. Stilwell and S. M. Park, J. Electrochem. Soc. 135 (1988) 2254.
[12]   D. E. Stilwell and S. M. Park, ibid. 135 (1988) 2491.
[13]   W. S. Huang, B. D. Humphrey and A. G. MacDiarmid, J. Chem. Soc., Faraday Trans. 1, 82 (1986) 2385.
[14]   W. W. Focke, G. E. Wnek and Y. Wei, J. Phys. Chem. 91 (1987) 5813.
[15]   J. C. Lacroix and A. F. Diaz, ibid. 135 (1988) 1457.
[16]   D. E. Stilwell and S. M. Park, ibid. 135 (1988) 2497.
[17]   S. K. Dhawan and D. C. Trivedi, J. Appl. Electrochem. 22 (1992) 563.
[18]   E. M. Genies, M. L. Lapkowski and J. F. Penneau, J. Elec-troanal. Chem. 249 (1988) 97.
[19]   D. M. Mohilner, R. N. Adams and W. J. Argersinger, J. Am. Chem. Soc. 84 (1962) 3618.
[20]   E. Galus and R. N. Adams, ibid. 84 (1962) 2061.
[21]   J. Bacon and R. N. Adams, ibid. 90 (1968) 6596.
[22]   Y. Wei, Y. Sun and X. Tang, J. Phys. Chem. 93 (1989) 4878.
[23]   V. Tsakova and A. Milchev, Electrochim. Acta 36 (1991) 1579.
[24]   P. Nunziante and G. Pistoia, ibid. 34 (1989) 223.
[25]   M. Gholamian and A. Contractor, J. Electroanal. Chem. 252 (1988) 291.
[26]   P. Herrasti and P. Ocon, J. Appl. Electrochem. 20 (1990) 640.
[27]   C. Mailhe-Randolph and J. Desilvestro, J. Electroanal. Chem. 262 (1989) 289.
[28]   S. Hackwood, W. C. Dautremont-Smith, G. Beni, L. M. Schiavone and J. L. Shay, J. Electrochem. Soc. 128 (1981) 1212.
[29]   T. C. Wen and C. C. Hu, ibid. 139 (1992) 2158.
[30]   S. Ardizzone, G. Fregonara and S. Trassatti, Electrochim. Acta 35 (1990) 263.
[31]   S. H. Glarum and J. H. Marshall, J. Electrochem. Soc. 134 (1987) 2160.
[32]   M. Lapkowski and E. M. Genies, J. Electroanal. Chem. 279 (1990) 157.
[33]   A. G. MacDiarmid, J. C. Chiang and A. F. Richter, Synth. Met. 18 (1987) 285.
[34]   R. L. Hand and R. F. Nelson, ibid. 125 (1978) 1059.
[35]   A. Lindenberger, In 'Electronic Properties of Polymers and Related Compounds' (edited by H. Kuzmary, M. Mehring and S. Roth), Springer-Verlag, New York (1985).